Ultrasonic Modification of Micelle Nanostructures

Nor Saadah Mohd Yusof and Muthupandian Ashokkumar

Contents

Abstract

The tremendous attention given to micelles in recent technological advancements and industries is due to its amazingly stable and flexible physicochemical properties exhibited upon exposure to different stimuli. A concise review of micelle

N.S. Mohd Yusof (✉)
Department of Chemistry, University of Malaya, Kuala Lumpur, Malaysia
e-mail: adah@um.edu.my; adah.yusof@gmail.com

M. Ashokkumar
School of Chemistry, The University of Melbourne, Melbourne, VIC, Australia

M. Ashokkumar (ed.), *Handbook of Ultrasonics and Sonochemistry*,
DOI 10.1007/978-981-287-278-4_18

structures and the effects of various stimuli on the structural properties of micelles with a particular focus on the effect of ultrasound are provided. While the use of conventional stimuli such as temperature, shear, etc., for controlling micelle structures is widely reported, the use of ultrasound as a stimulus has not been studied extensively. For this reason, a detailed discussion on the possibility of designing a variety of micelle nanostructures using ultrasound is provided. Using ultrasound as a stimulus is an advantage as it eliminates the need for adding external chemicals to the micellar system and the experimental parameters could be easily controlled. A case study of using cetyltrimethylammonium salicylate (CTASal) prepared from ion exchange process of equimolar mixture of cetyltrimethylammonium bromide (CTABr) and sodium salicylate (NaSal) is used in order to evaluate the efficiency of ultrasonics on controlling the micelles' aggregational structures. Further experiments and discussion imply that the transformation is mainly driven by the physical effect generated from sonication. Evidence from cryo-TEM indicates that the structural transformation took place according to the reptation and reaction Model proposed before.

Keywords
Micelle structure • Micellar aggregational reversibility • Viscoelasticity • Ultrasound-induced micelle

Introduction

Surfactant with unique characteristics of amphiphilicity can self-assemble to form micelles. When a low concentration of micelle-forming surfactant is dissolved in a solvent, surfactant molecules exist as monomers. Once the concentration reaches its critical micelle concentration or cmc, monomers aggregate together forming a "micelle." Micelle has the unique ability to flexibly break and reform within a wide range of sizes, from nm to mm, as well as to different aggregational structures with pronounced properties. Hence, they are also termed based on their structures such as vesicle, liposome, gel, microemulsions, etc. The amphiphilic behavior and the flexible aggregational properties make them very useful in many areas. People are more familiar with their areas of application such as soap, detergent, wetting agent, bactericide, corrosion inhibitor, foaming agent, dispersant, emulsifier, antistatic agent, and many more.

Micelle is a remarkable system because of its ability to undergo self-aggregational transformation even with the slightest change, such as settling in a different environment (solvent), increasing/decreasing its monomer's concentration, or even by slightly changing the solution temperature. Their assembly and transformational processes are a net effect from the balance of their electrostatic, hydrophobic, van der Waals, and steric interactions.

Micelle Aggregation

One of the earliest evidence for micelle aggregation was reported in 1913 by McBain who observed abnormal viscosity in sodium palmitate solution [1]. Despite its significant viscosity, the system still exhibited normal electrical mobility, therefore initially termed as "colloidal ion" [1]. The aggregation relied solely on the amphiphilicity of molecules (monomers) in the solution. In aqueous solutions, the water loving identity is exposed, and the water hating identity is well hidden in the core, a region where it is believed to be completely free of water molecules. In nonpolar solvents such as oil, the aggregation is reversed, hence termed as a reverse micelle.

The concept behind the aggregation of micelles is simple. In any system, each molecule stably exists in its lowest potential energy required. Conflict arises when both parts – water loving and hating are exposed to the solvent, i.e., water molecules. Hence, this molecule has no option other than orienting its water hating part at the air-water interface with the tail projected away from the water. However, as a collective system, specifically above its critical micelle concentration (cmc) and Kraft temperature, they have a better option by aggregating together, known as the self-assembling process. Kraft temperature is the minimum temperature required for the surfactants to start aggregating to form micelle. At temperature below Kraft temperature, micelle will not form even at its high concentration. The hydrophilic heads form a shield to avoid any interaction or any close contact of their hydrophobic tails to water molecules, by an equilibrium process known as aggregation or micellization. This is shown by Eq. 1 where S represents the monomer and S_n represents the micelle. By forming micelle, they possess lower potential energy; therefore the aggregation is very stable.

$$nS \rightleftarrows S_n \tag{1}$$

Despite the use of the term "stable", it is important to understand that micellization itself is a dynamic process of formation and deformation of micelle-forming surfactant monomers, as illustrated in Fig. 1. This is described by the micelles' equilibrium (K_M) in Eq. 2 where k_f^M is the rate constant of micelle formation and k_d^M is the rate constant of micelle deformation.

$$K_M = k_f^M / k_d^M \tag{2}$$

A micelle can flexibly and reversibly grow to different structures in order to stay in its lowest energy state. For deeper understanding, two crucial governing factors are discussed below [2, 3]:

(i) Any course of increasing the tail-tail attraction will lower the cmc as well as promoting growth, vice versa.

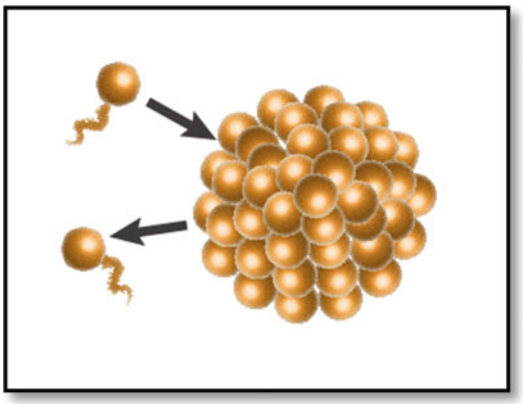

Fig. 1 Micellization process from monomers above cmc and Kraft temperature

- Hydrophobic group – micelle-forming surfactant with a more hydrophobic nature will result in stronger attraction, therefore has a low cmc and promotes growth.
- The number of carbon atoms building a straight chain – more carbon atoms in a straight chain will increase the hydrophobicity of the molecule.
- Branched carbon chain – with the same number of carbon atoms, increasing branch(es) will increase the cmc. This is because the potential energy of branched micelle-forming surfactant aggregation is higher than the corresponding linear molecule.

(ii) Any course of decreasing the head-head repulsion will lower the cmc and promote growth, vice versa.

- Charge(s) of the head – increase in the head's charge(s) will result in a greater repulsion between them, resulting in a higher cmc.
- Number of hydrophilic group – increase in the hydrophilicity will also result in an increase in repulsion between the heads, resulting in a higher cmc.
- Electrolyte and nonelectrolyte additives – any additive that can reduce the head-head repulsion will reduce the cmc.

In concluding terms, micelles' structural aggregation relies heavily on hydrophobic attraction but limited by the repulsion between hydrophilic heads. The balance between these two results in a curvature growth in order to gain more space between the charged heads, hence the formation of spherical micelles above the cmc. Despite the repulsion of the heads, surfactant molecules are closely packed together to ensure that its hydrophobic core is free of water. Therefore, in examining such aggregation, the terms of "spontaneous curvature" or "critical packing" (CP) behaviors are usually used for discussion [4]. Optimum head group spacing and water-free hydrophobic core will promote growth and determine the flexible structure of micelle. The average length of micelle is also known as its contour length, denoted by $\bar{L}$.

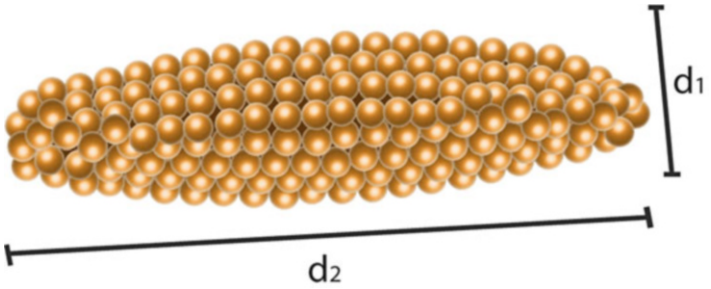

Fig. 2 The critical packing (*CP*) value is given by the ratio of the two diameters of the structure, d_1 and d_2

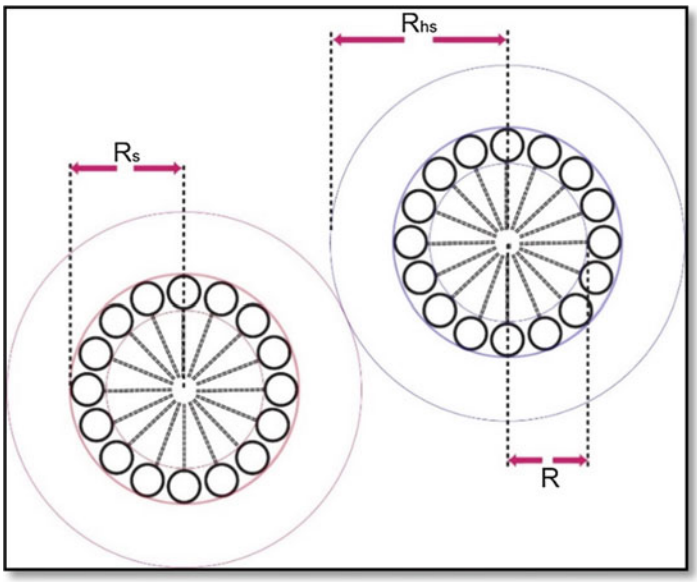

Fig. 3 The core radius (R), the shell radius (R_s), and the hard-sphere interaction radius (R_{hs}) of micellar aggregations in aqueous system

Micelle Aggregational Structures

Micelles can assemble by noncovalent interaction to different structures that are "energetically stable." The size of the aggregation can be described by their radii – the core radius (R), shell radius (R_S), and the hard-sphere interaction radius (R_{hs}) as shown in Fig. 3 [5]. However, when micelles grow (elongate), the critical packing (CP) process is usually described by the aspect ratio of the two diameters of the

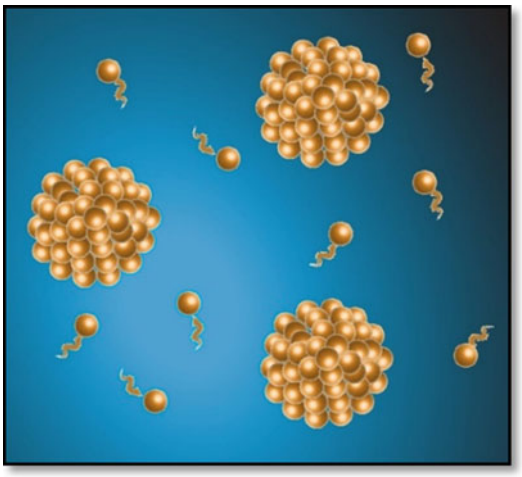

Fig. 4 Illustration of spherical micelles

structure, d_1 and d_2 in Fig. 2 [6]. This highly relies upon the required energy to form the curvatures that determine the two diameters of a micelle aggregation, which is also known as the scission energy [7]. The two diameters are the horizontal and vertical diameters of a micelle structure.

In simple cases where there is no external disturbance on the system, the scission energy depends solely on the strength of surfactant-counterion interaction [7]. When there are more than one counterions present, the strength is also characterized by the ion exchange constant, K^X_Y (X and Y are the two competing counterions) value [8, 9]. This and the surfactant-counterion ratio have significant effect on the system's viscoelasticity [10]. The length of the micelle's structure is usually determined by direct visualization of cryo-TEM imaging [11], or determination by light and neutron scattering [12, 13]. As micelles can form many aggregational structures, some of the common ones are mentioned in this section.

Spherical Micelles

The most common structure of micelle aggregation usually formed right above its cmc and Kraft temperature is the spherical micelle. As its name infers, they form more or less a sphere structure as illustrated in Fig. 4.

Since they form immediately above their cmc, the size is remarkably homogenous throughout the system, with its radius being approximately equal to the hydrocarbon chain length of its monomer. The CP for this structure is $\leq 1/3$ [4]. The curvature growth of the micelle is due to its adaptation to two factors: providing more space for the strong repulsion effect between the charged heads and aiding the strong attraction between the hydrophobic chains of its core. Spherical micelle solution does not show any significant viscosity increase but usually exhibits shear-thinning rheological property.

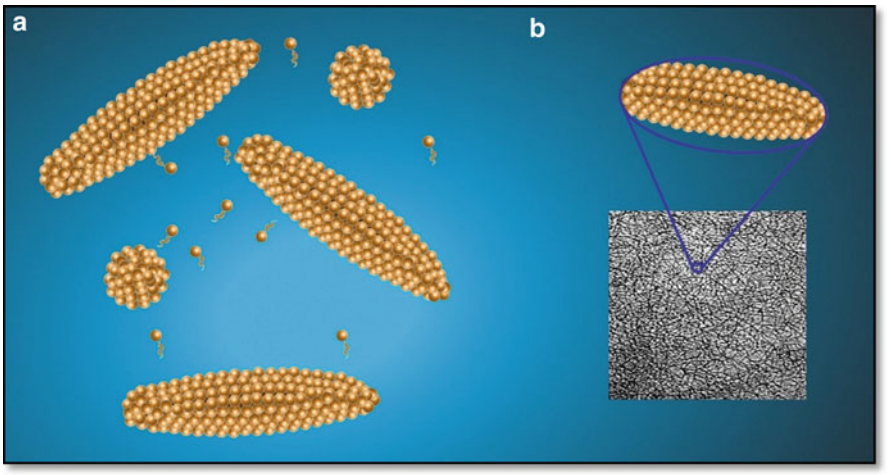

Fig. 5 Illustration of (**a**) rodlike and (**b**) wormlike micelles. Rodlike micelle is elongated micelle but does not entangle in a network. Wormlike micelle is much longer than rodlike micelle and entangled together

Rodlike and Wormlike Micelles

Within $1/3 \leq CP \leq 1/2$, a micelle can grow to rodlike or wormlike micelle as shown in Fig. 5 [4]. Such growth occurs by the natural act of the micelle aggregation process in order to reduce its total energetics by decreasing the proportion of its end caps over the linear portion [4]. This can only happen when energy for the spontaneous curvature of the end caps is higher than the energy of the curvature along its cylindrical structure. Compared to a spherical micelle, the core and shell radii of wormlike micelle is smaller [5]. The spherical micelle form rodlike micelle by its one-directional growth and continue to elongate depending on the condition [5].

The wormlike micelles tend to entangle together into a transient network. This entanglement results in its viscoelastic property [14]. Each of the wormlike micelle continues to break and reform either by itself or by interaction with its neighboring micelles within milliseconds timescale [15–17]. There have been many studies on such structures, due to their applications in many areas [17]. Researchers are mainly interested in the architecture of this structure because of its unique and beneficial reversible and flexible viscoelasticity.

Vesicles and Multilamellar

Lamellar structure is formed by fine alternating layers of different materials, or in the case of micelle aggregation are the alternating hydrophilic and hydrophobic layers as shown in Fig. 6b. When they form unilamellar structure with a hollow core, it is known as vesicle as in Fig. 6a. This kind of aggregation occurs when its $CP \geq 1/2$ [4].

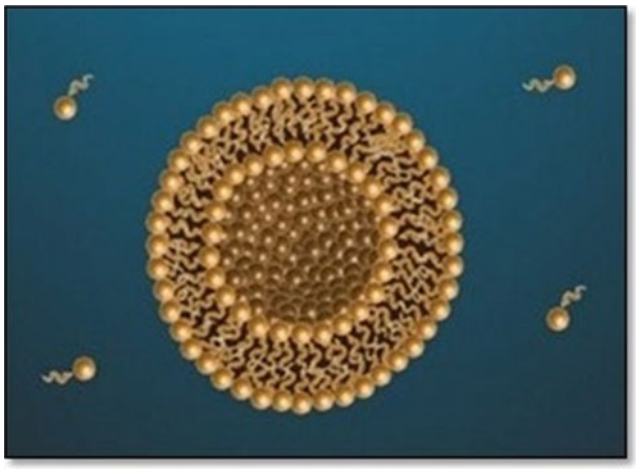

Fig. 6 Illustration of a vesicle

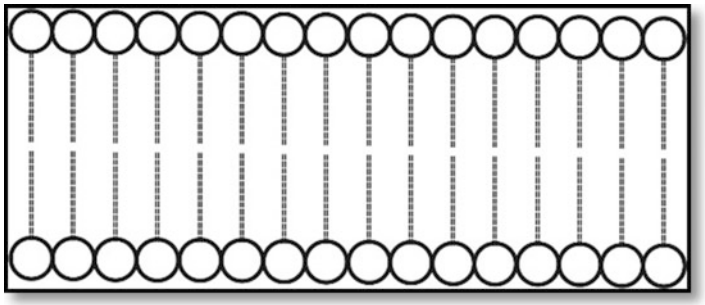

Fig. 7 A bilayer system formed by micelle forming surfactant

If the molecular assembly process is solely governed by the hydrophobic attraction, the monomers would prefer to aggregate to form a bilayer structure as shown in Fig. 7. However, due to the strength of hydrophilic repulsion of the hydrophilic head groups, the bilayer folds to form a vesicle with expected number of monomers to be less in the inner layer compared to the outer layer. This type of assembly can only form when the hydrophobic interaction is relatively much stronger than the head groups' repulsion. However, the inner heads are still assumed to be very closely packed. Transformation of micelle structure from wormlike micelle to vesicle can be easily detected by the significant and sudden viscosity reduction.

There has been many reports on micelle structural changes according to the order of the structures discussed above – monomer to spherical to rodlike/cylindrical to wormlike and to vesicle. In a simple system, e.g., the addition of strong binding counterions to a micelle solution can induce the aforementioned structural transformation. An example is the mixture of cetyltrimethylammonium bromide and

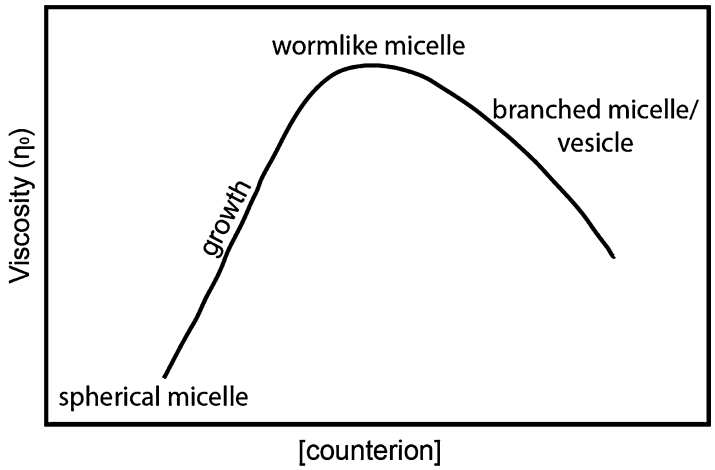

Fig. 8 The zero shear viscosity (η_0) of a micelle system upon increasing concentration of its counterion

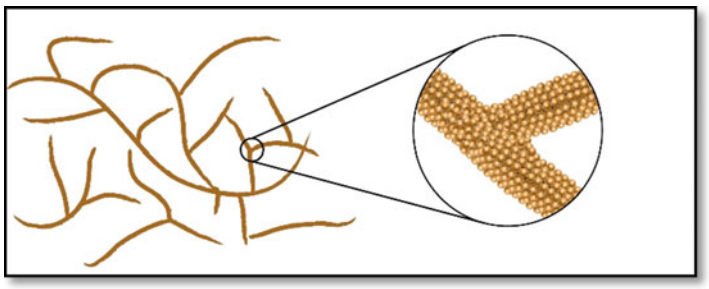

Fig. 9 Illustration of a branched micelle system

5-methylsalicylate [18]. Typically, this is detected by the viscosity measurement upon increasing counterion concentration as shown in Fig. 8.

There have been many studies that reported the formation of branched micelles (Fig. 9) instead of vesicles [2, 3, 19–25]. The branched micelle was found to exhibit a reduction in its viscosity value compared to the system of linear entangled wormlike micelle (Fig. 9).

The appearance of the branches in a micelle system is the way for a micelle to compensate the increase of its end cap energy, therefore having a mean curvature at the opposite direction of the original end caps [3, 5]. This is as a result of reptation reaction mechanism which will be explained in detail later. These intermicellar junctions have the ability to slide/diffuse effectively along the micelles' curvature length to release the stress also known as the relaxation process. This existence of this structure can only be confirmed by cryo-TEM imaging [2, 10].

Microstructural Transformation of Micelle

Micelle aggregational responses toward different stimuli have been studied extensively since the discovery of its viscoelasticity in the 1970s. The viscoelasticity of micelle system is a result from the aggregation forming wormlike micelles. Initially, such aggregational structure was formed at very high concentrations of surfactant. In 1976, it was first discovered that wormlike micelle structure can also be induced at surfactant's low concentration by adding certain additive such as salicylate and chlorobenzoates [26]. This discovery is not only beneficial due to the need of much lower concentration in achieving viscoelasticity, but it also contributes to unfolding the mystery of micelles' aggregational behavior. Eversince, the effect of other stimuli such as temperature, shear, UV-light, and solution pH were discovered to be able to induce micellar structural transformation. Since sonication will also result in the increase of temperature as well as generation of strong shear, these two stimuli will be briefly reviewed as below.

Temperature

In 1996, the ability of temperature change to induce micelle structural transition was first reported [27]. The system used was a mixture between CTAB and sodium hydroxynaphthalene carboxylate (SHNC) forming cetyltrimethylammonium hydroxynaphthalene carboxylate (CTAHNC). Upon temperature change from room temperature to 70 °C, vesicle (diameter = 1–10 μm [28]) to wormlike micelle transition was observed. This may be explained as below. At lower temperatures, the hydroxynaphthalene carboxylate (HNC^-) counter ion shows weak solubility in water. Therefore, it binds strongly to the CTA^+ (from CTAB) micelles' palisade layer resulting in the formation of vesicles. At higher temperatures, the solubility of the HNC^- increases, which then results in the two forms present: bound (HNC^-_{mic}) and unbound (HNC^-_{aq}). With less counterion binding in the micelle phase, the vesicles transform to wormlike micelle system. Similar observation was reported with the existence of salicylate ions [27]. Another example is the temperature effect on the cmc of a nonionic micelle system – the Tween surfactant series [29]. Its cmc was found to decrease with the increasing temperature up to 57 °C and slightly increase with further increase in temperature.

Shear

A year after the first discovery of the effects of temperature on micelle system, the effect of shear on the same micelle system was reported by Mendes et al. [30] Similar to the previous case, almost all of the vesicles transformed to wormlike micelle structure upon subjected to shear. This is usually evident by the increasing viscosity of the system. The appearance of shear induced structure (SIS) is also an indication of its response toward shear [7]. SIS can be clearly observed from shear thickening

rheological behavior in a flow curve plot. There are three stages involved in shear thickening of micelles: (i) induction; (ii) aggregation; and (iii) orientation [31]. However, such SIS phase is usually unstable and will relax to its original structure after a short period of time [32]. Unlike the system reported by Mendes et al., which was stable [30]. With shear applied, the micelle is stretched or extended. Therefore, the probability of their intermicellar interactions increases compared to its original state [33]. With sufficient shear, the scission energy can be overcome and the end caps will be broken, resulting in micelles with residual charges [7]. The micelles with residual charges then combine to form longer structure of micelle system [33].

Another example of vesicle to entangled wormlike micelle transition by the effect of shear was reported by Zheng et al. on cetyltrimethylammonium chloride (CTAC) and 3-methyl salicylate ion (CH_3Sal^-) [34]. The aim of the study was to imitate the blotting flow deformation process in the preparation cryo-TEM sample. Initially, the CH_3Sal^- counterions intercalated at the vesicle/water interface. As a strongly binding counterion, CH_3Sal^- is an effective species in reducing the electrostatic repulsion effect between the CTA^+ head groups and promotes the formation of vesicle. In flow field, the straining deformation of the experiment disrupted vesicle structure and altered the distribution of CH_3Sal^- counterions around the fragments of vesicles. This fragmentation is known as the vesicle division. The formation and dissociation in micelle equilibrium is now shifted, therefore altering the local preferred curvature of the aggregation. This initiates aggregational instability of the vesicles' fragments which then induces their reconstruction into the entangled wormlike micelle structure.

Ultrasonics and Micelles

The effect of ultrasound on micelle structure is an area that has not been investigated in detail. Though the propagation of ultrasound in a solution results in acoustic cavitation that generates extreme temperature and strong shear, the effect is more complex than simply applying heat and shear. Therefore, it is essential to study the effect of ultrasound on micelle system. One of the related publications reported in the literature is a study by Wang et al. [35] in 2009 on an amphiphilic diblock copolymer micelle system of poly(ethylene oxide)-*block*-poly(2-tetrahydropyranyl methacrylate) (PEO-*b*-PTHPMA). The ultrasound used in this study was a high-intensity focused ultrasound (HIFU) system operated at 1.1 kHz frequency and 200 W. The ultrasound system used was similar to the one used in therapeutic medicine. The choice of using PEO-*b*-PTHMA micelle is based on its sensitivity toward low pH condition and to thermal effect by hydrolysis process. The PEO-*b*-PTHPMA was found to undergo lysis and converted to poly(methacrylic acid) (PMAA) upon sonication due to the hydrolysis-induced cleavage of tetrahydropyran-2-ol [35]. This was initially detected by the pH reduction of the solution and confirmed by infrared analysis, dynamic light scattering, atomic force microscopy, and fluorescent measurements. The extent of micelle disruption was found to be governed on the power of sonication, solution volume and the size, as well as the location of the

targeted focal area on the system. Upon detailed study, they also reported that such observation did not take place in control experiments where no ultrasound was introduced, instead the solution was just heated at 90 °C, or just vigorously stirred for 4 hours. Therefore, they suggested that the phenomenon observed in their study was not purely the effect of heat generated, but also initiated by the mechanical effect of sonication. The effect of ultrasound in the study discussed above is mainly due to its ability in breaking the monomer forming the micelle system, instead of rearranging the monomers. This can be useful for designing drug delivery system [36, 37] given that none of sonicated product is dangerous to the human body.

This is followed by another publication on micelle structural change upon sonication on a catanionic (cationic/anionic) system of CTAB and 1-butyl-3-methylimidazolium octyl sulfate (Cmim) by Ghosh et al. [38] Pure Cmim in aqueous solution forms tiny micellar aggregation at around 3 nm in size [39]. However, once CTAB was introduced at different fraction, χ_{CTAB} ($\chi_{CTAB} = (V_{CTAB})/(V_{CTAB} + V_{Cmim})$), different types of micelle aggregational structures appeared, evident by the changes in the turbidity and appearance of the solutions. A similar observation has been reported before. A mixture of cationic and anionic micelle usually results in a neutral micelle assembly at equimolar mixing [40]. For mixtures other than their equal ratio, there will be excess charge that may spontaneously induce the formation of different sizes of vesicles [41, 42], independent of their formation path [43].

In this study, at χ_{CTAB} below 0.25, the solution was clear and possessed low viscosity, due to the existence of small micelles of pure Cmim and those mixed micelles formed by mixture with CTAB. However, at $\chi_{CTAB} = 0.25–0.6$, the system appeared to be bluish in color and showed turbidity behavior. This indicates the aggregation of vesicles in the system. At $\chi_{CTAB} = 0.6$, they reported the formation of large multilamellar vesicles with their size around 200–400 nm as evident by TEM images. The aggregation was described as an onion-like arrangement consisting of several concentric bilayers. From $\chi_{CTAB} = 0.7–0.8$, the system forms elongated micelle with viscoelastic property and above 0.8 they seemed to revert back to a clear micellar phase. Samples at $\chi_{CTAB} = 0.6$ was then further treated for spectroscopic study. The system was put under a few cycles of freezing and thawing and later sonicated using an ultrasonic probe for 20 min. The sonication was able to break the multilayer arrangement, resulting in the formation of a single layer vesicle in the size range of 90–125 nm [38].

Despite the interesting structural changes reported in this study, it only focuses on the ability of ultrasound to break micellar structure as reported by Wang et al. [35]. In addition, none of these publications discussed the mechanism of micelle structural changes (disruption) by ultrasound.

Ultrasound-Induced Structural Transformation of CTASal Micelle

The ability of ultrasound as a stimulus to induce micelles' microstructural transformation was recently investigated. In the study, the micelle system used was cetyltrimethylammonium salicylate (CTASal), prepared by an ion exchange process

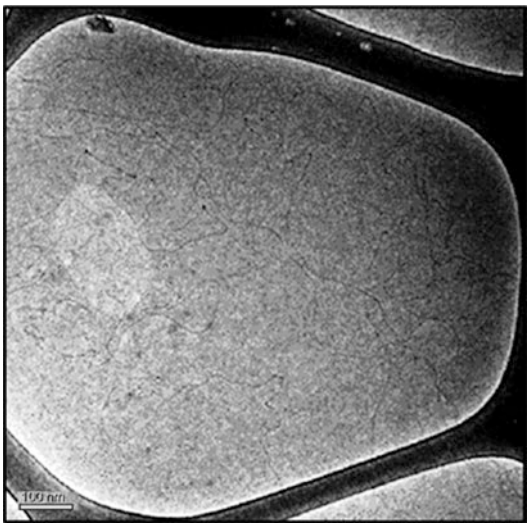

Fig. 10 Cryo-TEM image of CTASal micelle structures before sonication (Reproduced from Ref. [44] with permission from the Royal Society of Chemistry)

between cetyltrimethylammonium bromide (CTAB) and sodium salicylate (NaSal). A mixture of CTAB and NaSal was chosen over the commercially available CTASal due to the following reason. The existence of two counterions, i.e., bromide and salicylate ions would provide a better stability to the micelle system formed thereby inducing the formation of wormlike micelle even at lower concentrations. The effect of sonication on CTASal was investigated in the sonication frequency range of 20–1080 kHz and at applied power levels in the range of 10–70 W. Wormlike micelle structure was chosen by fixing the concentration ratio of 0.015 M CTAB and NaSal. The formation of wormlike micelle structure is evident from cryo-TEM imaging as shown in Fig. 10.

In addition, the effect of different sonication reactors on the CTASal micelle system has also been investigated. The reactors used were horn-, plate- and high-intensity focused ultrasound (HIFU)- type transducers. All three systems delivers different powers and from different directions. Horn and plate type transducers are standard commercially available units. However, the HIFU transducer used was custom built. The schematics of the three transducers are shown in Fig. 11.

The horn-type sonication reactor used was a Branson cell disruptor Model 450D. The frequency of this unit was 20 kHz with a maximum power output of 400 W. As shown in Fig. 11 (left), the ultrasound wave propagates through the medium from the horn transducer from the top direction. Since the depth of the transducer can be adjusted, the position was fixed throughout the experiment. The diameter of the horn used was 1 cm. The plate-type transducer used was an Allied Signal plate transducer combined with the ELAC RF generator. This is shown in Fig. 12. Four sets of transducers were used in order to vary the ultrasonic frequencies at 211, 355, 647, and 1080 kHz. The maximum applied power for this type of transducer was 100 W. For the purpose of comparing the frequencies, the applied power was fixed at

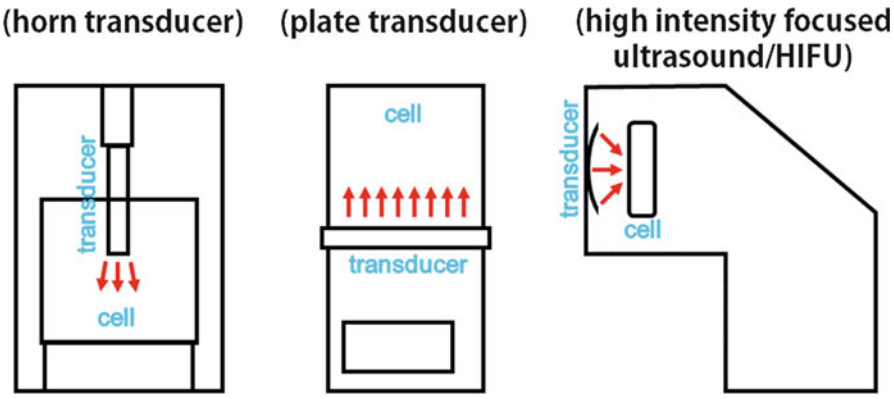

Fig. 11 The three ultrasonic reactors used in the study – horn-type transducer on the *left*, plate-type transducer in the *middle*, and high-intensity focused ultrasound (*HIFU*) on the *right*

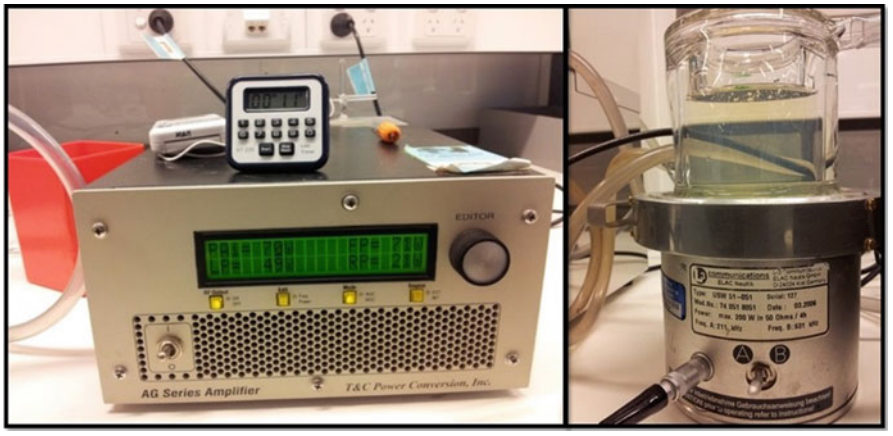

Fig. 12 The experimental setup of the sonication with the plate-type transducer. *Left*: function generator and amplifier; *Right*: transducer and glass cell

40 W. However, for the purpose of comparing the applied sonication power, few sets of experiments were carried out at 10, 40, and 70 W at 355 kHz.

For both transducers – the horn- and plate-type, 200 mL of micelle solution was used. The absorbed acoustic powers were measured by a calorimetric technique for all systems. The temperature of the experiments were maintained at 30 °C using a thermostated water jacket. Cryo-TEM images were taken for the sonicated micelle systems using a TF30 Transmission Electron Microscope from Tecnai, Heindoven, the Netherlands. The cryogenic treatment was essential due to the reversible nature of a micelle system. This will be discussed later. The rheological experiment was done using an AR-G2 Controlled Stress Rheometer from Anton Paar.

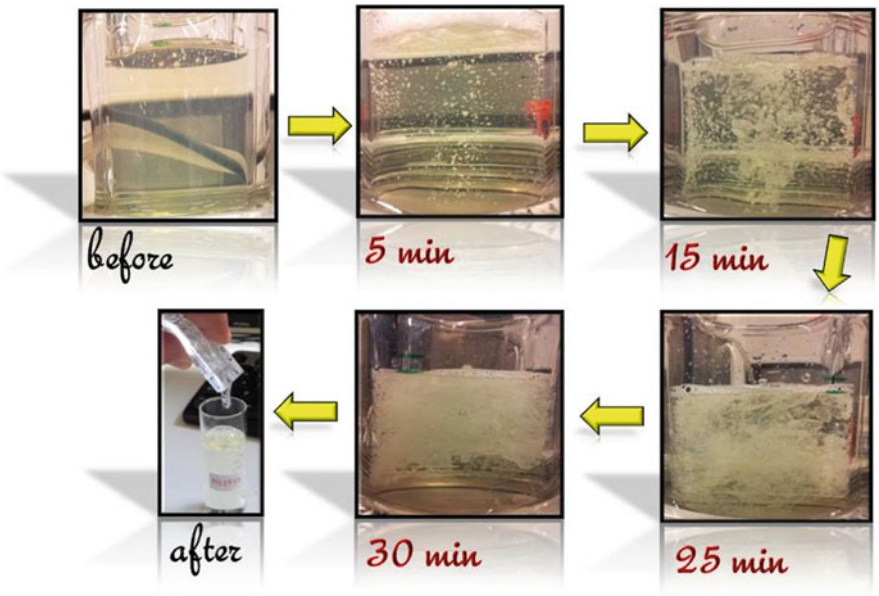

Fig. 13 The pictures of micelle solution over sonication time. The solution was homogenous before sonication started. When sonication started, small micelle agglomerates appeared and adhered together with increasing sonication time. This lead to the separated two layers of micelle system when sonication was stopped. The after image was taken during the transfer of the top layer from one cell to another (Reproduced from Ref. [44] with permission from the Royal Society of Chemistry)

Sonication at 211 kHz Frequency and 40 W Power

The first set of experiment was carried out using the plate-type transducer at 211 kHz frequency and 40 W of power. Upon sonication, the homogeneous micellar solution was transformed into two separated layers of micelle system with significant difference in their viscoelasticity. This is shown in the pictures taken at different sonication times in Fig. 13. The first image was taken for the micelle solution before sonication experiment. It was left overnight for equilibration. Within the first few minutes of sonication, the micelle agglomerates were visible and agglomeration increased with an increase in sonication time. These individual aggregates adhered together leading to phase separation. The two layers stayed separated when sonication was stopped. The aforementioned changes in were absent when blank experiments were carried out without ultrasonic irradiation, instead only with shear effect caused by stirring a magnetic stirrer. Therefore, it can be concluded that such changes were induced by sonication effect. By initial visual observation, the top layer of the sonicated micelle system was showing strong viscoelasticity. On the other hand, the bottom layer showed a water-like viscosity. The opaque top micelle

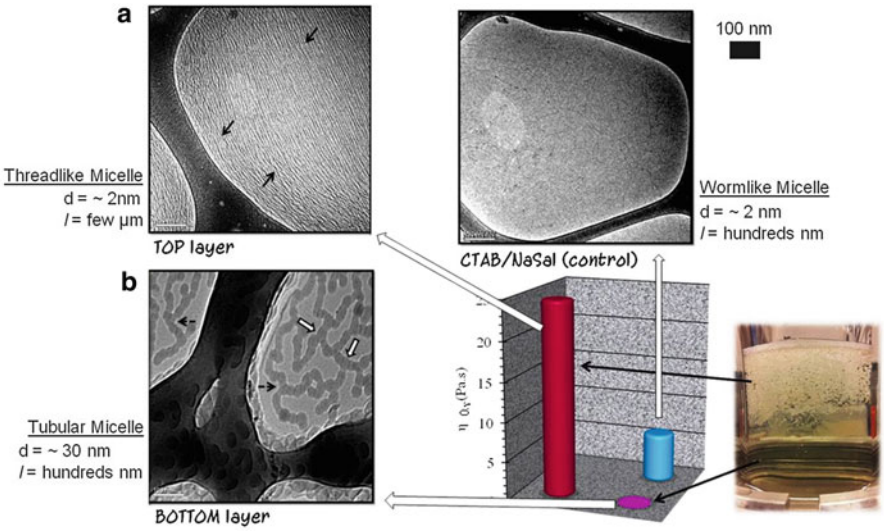

Fig. 14 The viscosity values and cryo-TEM images of CTASal micelle system before sonication and for the both top and bottom layers after sonication (Reproduced from Ref. [44] with permission from the Royal Society of Chemistry)

layer and the bottom, smaller aggregates in the aqueous micelle system were analyzed to determine their aggregational structure and viscoelasticity property.

The viscosity result and cryo-TEM images of the micelle system for both layers are presented in Fig. 14. The viscosity of the CTASal micelle system before sonication was measured to be around 6 Pa.s. However, after sonication, the top layer of the micelle system was found to exhibit viscosity value for almost four times greater (22.7 Pa.s) than that of before sonication and the bottom layer was found to exhibit more than 100 times less viscosity (0.04 Pa.s). The high viscosity shown for the top layer is due to the structural transformation of initial wormlike micelle to long and stable threadlike micelles. These micelles entangled together by the force of ultrasound from the plate transducer. On the other hand, the low viscosity observed of the sonicated bottom layer is due to the formation of vesicles and tubular micelles. The significant difference of viscoelasticity can be properly explained by looking at their cryo-TEM images.

Upon cryo-TEM imaging, it was found that the wormlike micelle initially formed by CTASal solution underwent significant transformation during sonication. The top layer of the sonicated micelle formed a very long threadlike micelle structure, thence exhibiting higher viscoelasticity. The structure has a diameter of ~2 nm and length of several µm. This was determined by examining the end caps of the micelles seen on the images. On the contrary, tubular micelles were observed at the bottom layer of the sonicated micelle system, thence the water-like viscosity shown. The diameter of the micelle is ~30 nm with a length of a few hundred nanometers.

With detailed inspection of the images, some important characteristics of micelle displayed can be detected. The long threadlike micelles formed in the top layer were

greatly aligned. The cause of this is sonication, rather than other factors during sample preparation. Despite being almost completely aligned, the occurrence of bond interchange between the individual micelles are obvious from the four-armed star junction points shown by the black arrows in Fig. 14. On the other hand, close examination of the tubular micelle in the bottom layer of sonicated micelle revealed that the tubular structure is due to the coalescence of vesicles in the system. At a given magnification, the coalesced vesicles building a tubular micelle can be clearly seen. The interaction results in the structure of tubular micelle with T-shape (white arrow) and Y-shape (dashed arrow) junctions. Some of the vesicles are still visible in the cryo-TEM images. Some examples are shown by the black circle in Fig. 14. This is due to the reversed process of tubular micelle formation caused by the effect of shear during the blotting process of the sample preparation. The process of vesicle coalescence takes a longer time than the relaxation of aligned micelles. This also indicates that the coalesced vesicles in this form are intermediates rather than stable structures. The detailed information revealed from cryo-TEM images will help in proposing the structural transformation of the micelle system to be discussed later.

Micellar Structural Transformation

The structural transformation of micelle as observed in the case study above may offer a great possibility in many technological advancement and improvements in industries. Despite the many discoveries of micelle structural responses toward different stimuli, the mechanism was never discussed in detail. In 1980s, early attempts to propose a theory for micelle transformation was done based on polymer system. However, due to significant difference of rigidity between polymer and micelle system, Cates came up with a refined theory in 1987 known as the Reptation Theory [45]. The model was refined by taking into account the continuous reptation and breakage of individual micelle [46]. The overview of micelle reptational and breakage processes are reviewed in this section.

Reptation Model

The resemblance of a system of elongated micelles, especially the entangled worm-like micelle to polymers has been proposed before, evidenced by the emerging publications on the analogy between these two [21]. Their appearance similarity emanate relaxation mechanism theory for micelle systems adapted from the well-known relaxation theory of polymers [45]. According to the original theory for a polymer in melt, the stress relaxation process of the polymer relies on the reptational diffusion of its long linear chains [45, 47]. This is a process when any given chain in a semidilute system gradually disentangles from its neighboring chains which creates a tube-like environment by diffusing along its own curvilinear silhouette [47]. The relaxation of the reptation process is given by Eq. 3. $\bar{L}$ is the fixed length of the particular polymer chain and D_0 is its mobility constant.

$$\tau_{rep} = \dot{L}^{\overline{3}}/D_0 \tag{3}$$

According to the reptation theory for polymers, the self-diffusion coefficient has a direct influence to its aggregational property, according to Eq. 4 below. D_S is the self-diffusion coefficient, N is the number of monomers per chain, and c is the concentration of the monomer [46, 48].

$$D_S \propto N^{-2}c^{-1.75} \tag{4}$$

In such discussion, the polydisperse distribution focuses on its mean value, N_0, and is known to increase with the monomer's concentration according to the Eq. 5 [46].

$$N_0 \propto c^{0.5} \tag{5}$$

However, Eq. 5 is only true in an ideal case, when the interactions between the chains are completely ignored. Thus, the equation was later simplified as Eq. 6 [49].

$$N_0 \propto c \tag{6}$$

Therefore, from Eq. 6, the polydispersity distribution is represented in Eq. 7.

$$D_S \propto c^{-3.75} \tag{7}$$

However, in contrast to a polymer, micelle is a dynamic system with its ability to continuously break/dissociate and reform at equilibrium, K_M [45]. These processes are represented by Eq. 8. In this equation, k_f is the rate of micelle formation and k_d is the rate of micelle deformation.

$$K_M = k_f / k_d \tag{8}$$

The micelle formed undergo a reversible exchange of its monomers [50]. Due to this characteristic, such spontaneously formed system of elongated micelle has also been described as a type of "living polymer," examples include CTAB/KBr (cetyltrimethylammonium bromide/sodium bromide) and CTAC/NaSal (cetyltrimethylammonium chloride/sodium salicylate) [21, 51–53]. Micelle is also very different than a polymer in its number of monomers per aggregation or aggregational unit. Unlike a polymer, the length of a micelle chain will continuously change depending on many internal and external factors such as its concentration, additive(s) existence, and other stimuli. In realization to this, Cates proposed the modified relaxation theory of micelle in 1987 by taking into account its dynamic properties. Following the discussion, he has outlined a few kinetic assumptions of micelles' breaking and recombination processes as below [45]:

(i) A micelle chain can break with a fixed probability per unit time per unit length at any part in the chemical sequence.

(ii) Reversed reaction or recombination of two chains occur with a rate proportional to the concentration of the product of the two reacting subchains.
(iii) Rate constant involved is independent of the molecular weights of these two subchains.
(iv) There is no higher probability for a chain end to link up with the chain from which it was recently detached than with any other chain end in the vicinity.

With the aforementioned rules in mind, the stress relaxation model revolves around two important time scales which are the τ_{rep} and τ_{break}. This is the main difference of micelle system as compared to polymers. The τ_{rep} represents the survival time for the classical reptation process of a chain within the micelle's contour length to occur before it disappears due to recombination. On the other hand, the τ_{break} is the survival time of a chain within $\bar{L}$ before it breaks into two independent chains [45, 46]. These two are highly influential for the related discussion as their balance determines the micelle system's harmony [45].

In cases that the reptation time is less than its breaking ($\tau_{rep} < \tau_{break}$), the principal of stress relaxation process of a micelle system is merely by reptation process. When τ_{rep} is much less than τ_{break}, ($\tau_{rep} << \tau_{break}$), along with the continuous reptation, the chain is essentially unbreakable [50]. In this condition, any possible reaction can be considered as impossible. The particular chain will diffuse along its curvilinear distance and become completely free from its original tube [50]. However, in a steady state of a dynamic equilibrium of a micelle system, a chain can break in any interim along its length, as well as it can recombine with another chain in a short time interval. Cates has outlined the two principals in micelles' relaxation mechanism [45]:

(i) The chain can break within a certain length traveled.
(ii) The curvilinear diffusion may bring the new chain end past before it recombines.

In this discussion, the interaction between micelles is equally important and cannot be overlooked. In addition, neighboring chains are also expected to alter their arrangements under the same time scale. Elongated micelles in a semidilute system are usually entangled and continuously interacting with each other. In understanding this, two popular models are usually used for discussion purpose: (i) tube model and (ii) breathing modes model. According to the tube model, the neighbors of a particular chain in an entanglement provide a tube-like steric constraint that restricts the diffusive motion as the chain moves [46, 47, 49, 50, 54]. This has been briefly mentioned as part of the discussion before. This chain can break with roughly equal probability per unit time in any point along its length. The recombination point relies smoothly on the chain lengths that, by detailed balance, the lifetime of a broken end before recombination (τ_{rep}) is comparable to the lifetime of the original chain before breaking (τ_{break}) [45]. On the other hand, when there is a fluctuation in its tube length, the tube is said to be in a "breathing mode" where it

stretches in the Rouse-like motion that is shorter than the entanglement length. In this case, reptation to a specific tube segment is not required, instead the process is faster by the breathing fluctuation process [45]. Both models are considered possible under specific condition in the micelle system. However, in many cases, tube model is used to ease the discussion. But, in many cases, the neighboring chains are also expected to alter their arrangements under the same time scale [45].

In another case that the reptational time is greater than its breaking, $\tau_{rep} > \tau_{break}$, the chain will break at a point close enough to a given segment of tube for reptative relaxation to occur before the new chain end is lost by recombination. In other words, the chain breakage and reformation occur often before it has disengaged from its tube by ordinary reptation. In this case, the time scale for the stress relaxation mechanism, τ_R is given by Eq. 9 [45].

$$\tau_R = \left(\tau_{rep} \bullet \tau_{break}\right)^{0.5} \tag{9}$$

When τ_{rep} is much greater than τ_{break}, $\tau_{rep} >> \tau_{break}$, the chain undergoes a number of breakages before it reptates out of its original tube [50]. This can be explained as below. As elucidated before, as the micelle is entangled in its semi dilute regime, each chain is constrained by a tube-like environment of its neighbors. With any small strain on the system, the particular micelle exists in nonequilibrium conformation or chaos and therefore induces the stress relaxation process. This takes place by the reptation diffusion process along its curvilinear length until the chain is out of its original tube, and enters a new tube, which at that point, is in equilibrium. At this point of the end of the chain, the particular micelle is said to be relaxed. From the discussion, even though the two time scales τ_{rep} and τ_{break} are important in understanding the stress relaxation mechanism of a micelle system; the stress relaxation time is simply represented by τ_{rep} [50]. The adsorbing ends of the chain segments make arbitrary jumps with appropriate transition probabilities or known as the recombination process.

Recombination of micelles can take place when two micelles come into contact with each other at some point with a sufficient energy available, such as the sudden change in the temperature or temperature jump in a system. There are three possible routes of recombination which are the reverse scission or end to end reaction, bond-interchange reaction, and the end-interchange reaction. Many factors were predicted to command any of the preferred routes between the three such as different chemical components, salinity, and temperature condition [50]. However, the discussion remains vague. The cases of all three possible recombination of micelles will be discussed separately in the section below. For the discussion, the breaking time of a micelle, τ_{break} is assumed to be independent of the concentration of surfactant and inversely vary with micellar length ($\tau_{break} \sim L^{-1}$) [45].

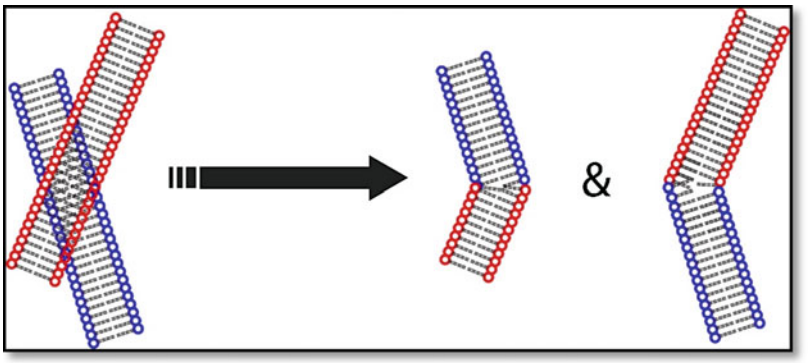

Fig. 15 Bond-interchange reaction between two elongated micelles

Reactions of Micelles

Bond-Interchange Reaction

Bond-interchange reaction is when two chains react and combine at some random point along their curvature length. This is evident by the appearance of a transient structure of a four-armed star junction, which can be detected by cryo-TEM imaging. This interaction results in the breaking of the structure to two new chains, with random exchange process of one part between the two of them. This is illustrated in Fig. 15. If this does not occur, both of them will break to form their original structures [50].

For bond-interchange reaction to occur, the timescale, τ_{break} is given by Eq. 10 where ϕ is the volume fraction of micelle and k_b is the rate constant [50].

$$\tau_{break} = \left(\phi \bar{L} k b\right)^{-1} \tag{10}$$

The τ_{break} is the supposedly needed time for one average chain to break. Considering the equilibrium of micelle aggregation as discussed before, τ_{break} is also comparable to the supposedly needed time for recombination reaction, τ_{rep}.

Even though the reaction is characterized by its rate constant, its overall rate is proportional to the square of its curvature length density. In this case, the lateral motion of the chains usually cannot be constrained by the entanglement of the system. Therefore, most of the time, through the bond-interchange reaction, micelle chain will pass through each other, or known as the "tube evaporation" process. In this unique process that cannot take place in polymer system, the entanglement of micelle is removed. Turner has summarized the relaxation time scale for different mechanisms of bond-interchange as Eq. 11 [50].

$$\begin{array}{ll} \tau_{rep} & \text{for } \zeta \geq 1, \text{ “unbreakable” chains} \\ \tau \approx \zeta^{1/3}\tau rep & \text{for } \alpha^{3/2} \leq \zeta \leq n1, \text{ reptative regime} \\ \alpha^{-2/5}\zeta^{3/5}\tau rep & \text{for } \alpha^{4} \leq \zeta \leq \alpha^{3/2}, \text{ breathing regime} \end{array} \quad (11)$$

And by scaling, the relationship of τ with its micellar volume fraction, ϕ is given by Eq. 12 [50].

$$\begin{array}{ll} \phi 3.4 & \text{for } \zeta \geq 1, \text{ “unbreakable” chains} \\ \tau \sim \phi 1.7 & \text{for } \alpha^{3/2} \leq \zeta \leq 1, \text{ reptative regime} \\ \phi 1.2 & \text{for } \alpha^{4} \leq \zeta \leq \alpha^{3/2}, \text{ breathing regime} \end{array} \quad (12)$$

The attempt frequency is highest for the bond-interchange process compared to the other two which will be discussed below. But its activation energy is also found to be higher compared to others.

End-Interchange Reaction

End-interchange reaction is when the end of the first micelle chain “attack” and combine with the second chain at its random point along its curvilinear length. In this case, a transitory three-armed star junction forms and then break to two new chains. The first chain combines with a section from the second chain, and another section from the second chain breaks as a new independent chain. This is illustrated in Fig. 16.

The timescale for this particular reaction is given in Eq. 13 where C_e is the chain's density and k_e is the rate constant for the end-interchange reaction process.

$$\tau_{break} = \left(C_e \dot{\bar{L}} k_e\right) - 1 = (\phi k_e)^{-1} \quad (13)$$

Even though the reaction is characterized by its rate constant, k_e, the overall rate is proportion to two parameters – the curvature length density and the density of end chains. The summary of the relaxation time scale for the different mechanisms of end-interchange reaction is shown in Eq. 14.

$$\begin{array}{ll} \tau_{rep} & \text{for } \zeta \geq 1, \text{ “unbreakable” chains} \\ \tau \approx \zeta^{1/2}\tau_{rep} & \text{for } \alpha \leq \zeta \leq 1, \text{ reptative regime} \\ \alpha^{-1/4}\zeta^{3/4}\tau_{rep} & \text{for } \alpha^{3} \leq \zeta \leq \alpha, \text{ breathing regime} \end{array} \quad (14)$$

And the relationship of τ with its micellar volume fraction, ϕ is given by Eq. 15 below.

$$\begin{array}{ll} \phi^{3.4} & \text{for } \zeta \geq 1, \text{ “unbreakable” chains} \\ \tau \sim \phi^{1.2} & \text{for } \alpha \leq \zeta \leq 1, \text{ reptative regime} \\ \phi^{0.58} & \text{for } \alpha^{3} \leq \zeta \leq \alpha, \text{ breathing regime} \end{array} \quad (15)$$

The attempt frequency of this mechanism is less than the frequency for bond-interchange mechanism, but more than the reverse scission which is explained below.

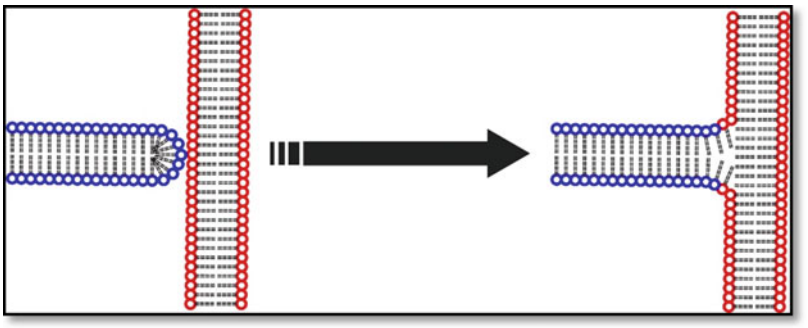

Fig. 16 End-interchange reaction

Fig. 17 Reversed scission or end to end reaction

Reverse Scission Reaction

Reverse scission reaction is when two micelles combine together at their ends thus sometimes termed as the end-to-end reaction. The bimolecular recombination reaction usually results in a longer linear unimolecular micellar chain. The reaction is illustrated in Fig. 17.

The timescale for this particular reaction is given in the Eq. 16 where k_s is its rate constant.

$$\tau_{break} = \left(\bar{L} k_s\right)^{-1} \tag{16}$$

For this reaction, k_s unit is per unit time per unit curvature length. However, it is speculated to be independent of its chain length.

The relationship of τ with its micellar volume fraction, ϕ is given by Eq. 17.

$$\tau \sim \begin{cases} \phi^{3.4} & \text{for } \zeta \geq 1, \text{ “unbreakable” chain} \\ \phi^{1.4} & \text{for } \alpha \leq \zeta \leq 1, \text{ reptative regime} \\ \phi^{0.88} & \text{for } \alpha^3 \leq \zeta \leq \alpha, \text{ breathing regime.} \end{cases} \tag{17}$$

The reverse scission reaction possess the lowest attempt frequency, but it also possesses much less activation energy as compared to bond-interchange and end-interchange reactions.

For all three cases, Turner has reported that the k_b, k_e, and k_s are independent on the chain length or concentration of micelle. Instead, they are highly dependent on the local motion of the chain's subsection [50]. It has also been reported that for the CTAB/KBr system, the temperature jump results only in reversible scission reaction.[50].

Mechanism

Based from the reptation and reaction model of micelle and the physical effects caused by sonication, the mechanism for ultrasound-induced structural transformation as observed in the case study of CTASal micelle is discussed in this section [44].

The propagation of ultrasound in liquid system causes a phenomenon known as the acoustic cavitation, which generates shear, heat, and reactive radicals upon bubble oscillation and implosion [55, 56]. In general, the physical forces generated during acoustic cavitation work according to the two categories – at "micro-" and "macro-" scales. The effect on the microscale is due to the cavitating and collapsing micron-sized bubbles at its antinodes. These processes generates strong shear due to the liquid system, known as the acoustic/cavitation microstreaming [55–57]. On the other hand, at the macroscale, the acoustic streaming pushes particles/materials in the system, causing separation of materials in accord to their sizes [58]. A number of theories have been proposed in describing the micellar structural transformation such as the reptation model of a polymeric micelle discussed in the section before [45, 59]. However, the explanations are considered as only speculations due to the missing experimental evidence at a molecular level. Therefore, the proposed mechanism for the case observed in this study in support of what was theoretically proposed earlier is crucial. Possible mechanisms of micelle structural changes are shown in Fig. 18.

The transitional processes are complementarily aided by the forces generated during sonication. IWM in Fig. 18 is the initial wormlike structure of CTASal that has been reported in earlier studies and shown in Fig. 10 of this book chapter [44]. LTM is the long threadlike micelle and TM is the tubular micelle structures observed for the top and bottom layers after sonication. The process of micellar aggregation to form long micelle structures is predicted to be similar to a polymerization process, but with the most important difference that the monomers continuously dissociate and reassociate forming a micelle structure [44, 45]. Due to this, unstable branching of micelles may form upon the changes in shear and temperature, and the micelles may revert back to the original IWM structure upon the removal of the stimuli. This is in contrast with the stable, aligned, very long threadlike micelles observed in the case study. In addition to the observation of these ultrasound-stimulated stable structures, the results also provide strong support to the reptation reaction model, which was initially proposed for polymer relaxation and extended by Cates [45] for wormlike micelles by considering the reversible breakdown and recombination of the structure [18, 60, 61]. Details of this model as according to the experimental evidence of the case studied are discussed below.

As shown in the mechanistic routes in Fig. 18, the nanostructural transition process starts with the entangled IWM prior to sonication at the center of the figure. As mentioned before, sonication results in the oscillation of microbubbles of different sizes from its minimum to maximum sizes, around less than 0.1–10 mm [62]. Some of these bubbles may be trapped in between the entangled IWM. The oscillation of these trapped microbubbles generates shear and acoustic microstreaming, which is favorable for the reptation process [45, 59]. According

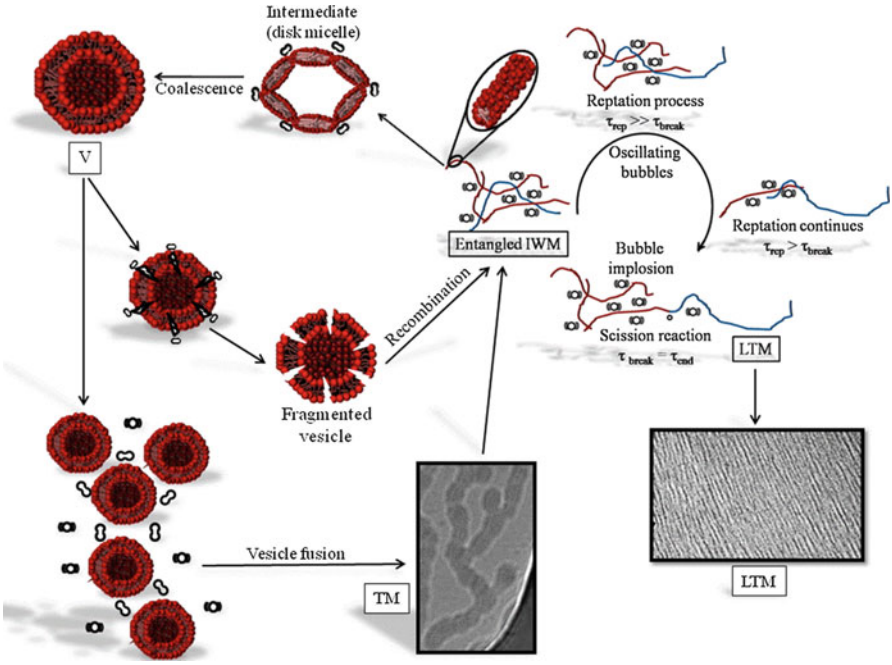

Fig. 18 The schematic illustration of the structural transitions of CTASal micelles from the initial wormlike structure to the long threadlike and tubular micelles (Reproduced from Ref. [44] with permission from the Royal Society of Chemistry)

to the reptation model of a micelle, the micelle forming surfactants may undergo reversible exchange reaction [59]. As reviewed earlier, the exchange reaction may take place by three means: (i) bond-interchange, (ii) end-interchange, and (iii) forward (scission) reactions. Bond interchange occurs when two wormlike micelles come into contact, break, and recombine as a four-armed star junction [50]. End-interchange reactions occur when the end of a wormlike micelle comes into contact with another wormlike micelle alongside, break and fuse to form a three-armed star junction [50]. This has not been observed in the case study. The forward reaction occurs when two wormlike micelles break at a random point along their length, reptate through and recombine at the end to end points of one another. Cates [45] has also mentioned that the highest probability of micelle interaction is the bond interchange reaction, however, the forward (scission) reaction possesses a much lower energy barrier compared to the other two reactions. The arguments put forward in this theory are fully supported by our experimental observations. The attempts for a bond interchange process are evident by the four-armed star junction. However, due to this structure being energetically unstable to recombine, the wormlike micelles continue to reptate through to be freed from the entanglement. This is majorly aided by the shear generated from microbubble oscillation. Mathematically, the process is due to the much larger relaxation time for the reptation process

compared to the relaxation process of the micelle breakage for recombination [50], thus reptation continues. In addition, the bubbles trapped in between the IWM achieve longer stability due to the IWM around them and continue to push the micelle free through reptation. As soon as the reptated micelle is released, the trapped bubbles are suddenly being freed from the entanglement and implode, inducing a temperature jump in the vicinity of the micelles, which causes the scission (end to end) reactions [26]. The breakage/recombination of micelles occur only when the reptation process finishes at the end of the micelles [50]. In other words, at the point when the ends of two micelles meet, breakage of the micelles occurs, which is followed by the recombination of the two of them. The whole process continues and results in the formation of LTM stabilized by the aligned patterned structure.

On the other hand, there is an equal probability of another case that the reptation process is agitated by a backward force from another oscillating bubble in the opposite direction, the micelles form a disk-like structure, which is known to be an intermediate to a vesicle [44]. The reorganization of disk micelles in a certain angle allows the bubbles to grow to their maximum size and collapse, resulting in a temperature jump in the vicinity of the micelles and recombination of the disk micelles forming vesicles (V). The vesicles then combine together forming tubular micelles™. The existence of TM agrees with the low viscosity but is higher than the viscosity of the vesicles, which is usually similar to water. TM is also known to be an intermediate in the structural transition process from vesicle to wormlike micelles as reported in the literature [35, 50]. From the above discussion, we may conclude that the processes shown at the right side of Fig. 18 build up the very viscoelastic top layer and the processes shown at the left side of Fig. 18 build up the less viscoelastic bottom layer as a function of sonication.

Sonication of CTASal Under Various Ultrasonic Conditions

A more comprehensive investigation on the effect of ultrasound frequency and power and the type of reactor on the structural changes was carried out [63]. Different structural responses were detected using rheological measurement and cryo-TEM images. These are shown in Table 1.

From Table 1, only sonication with plate-type transducers and at power more than 40 W resulted in the formation of two phases of micelle solutions with opposing degree of viscoelasticity. These two systems form separable layers and stay unmixed even after the sonication is stopped. The viscosity values and cryo-TEM images for these systems are shown in Figs. 19 and 20. For ease of discussion, Fig. 19 shows the experiments at different frequencies but at fixed power of 40 W, and Fig. 20 shows the experiments at different powers but at fixed frequency of 355 kHz.

Referring to the viscosity values in Fig. 20, it is clear that there is a decreasing viscosity trend with increasing frequency for the top layer system. On the contrary, an increasing viscosity was observed with increasing frequency for the bottom layer. To understand this, we need to examine the micelle structures formed in both layers,

Table 1 The effect of sonication parameters on the extent of micellar structural transformation

Transducer	Frequency	Power (W)	Phases(s)	η_0(Pa.s)	Micelles' structures
–	–	–	–	6.2	Wormlike micelle (control)
Horn (1 cm tip)	20	80	1	3.3	Rodlike micelle
Plate	211	40	2	24.7	Threadlike micelle
				0.1	Tubular micelle
	355	10	1	6.5	No change
		40	2	17.3	Threadlike micelle
				0.9	Tubular micelle
		70	2	21.0	Threadlike micelle
				1.0	Tubular micelle
	647	40	2	12.0	Threadlike micelle
				2.0	Tubular micelle
	1080	40	1	1.7	Vesicle
HIFU	643	10	1	4.9	Rodlike micelle
		40	1	4.3	Rodlike micelle
		70	1	4.3	Rodlike micelle

and understand the physical and chemical effects of sonication with increasing ultrasonic frequency along with the reference to the mechanism proposed.

Very long threadlike micelle structures were observed in the top layer for all three frequencies. They are ~2 nm in diameter and several μm in length. The cryo-TEM images for the threadlike micelles in all three systems seem to reveal some structural alignment. The threadlike micelle is the most aligned at 211 kHz and gets less coordinated with increasing frequency. The existence of tubular micelles can be seen from the cryo-TEM images of the bottom layers. The micelles are ~30–50 nm diameter and few hundred nm in length with the diameter increasing with the increasing frequency. At 211 kHz, despite the formation of the tubular micelle structure, the spherical shape of vesicle is still somehow visible, although not very clear. In other words, the micelle system forms a more stable tubular structure when sonicated at higher frequency. From sonication point of view, the wavelength is dependent on the ultrasonic frequency – longer at low frequency and shorter at high frequency. This results in the formation of larger microbubbles at low frequency when compared to those at higher frequencies. The oscillation of larger microbubbles results in the generation of relatively higher shear. As the frequency increases, microbubbles in the antinodes get smaller and generate relatively lower shear. Therefore, the shear decreases with increasing sonication frequency. According to the mechanism, the reptation of wormlike micelle is promoted by shear from the oscillating microbubbles. It seems logical that the threadlike micelle is the longest and most aligned at 211 kHz with highest viscoelasticity. To support the argument that the shear forces play a major role in causing changes to the structures and viscosity, let us look at the effect of sonication power. The shear is

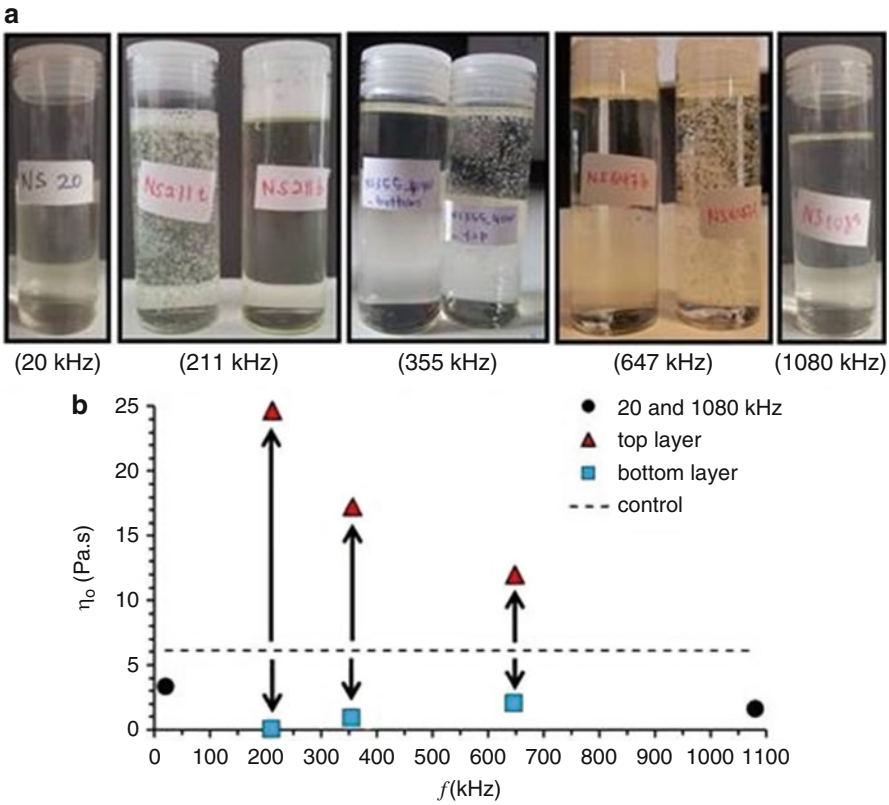

Fig. 19 (**a**) The top images are the sonicated CTASal micelle system at 20, 211, 355, 647, and 1080 kHz frequencies. 20 kHz uses horn-type transducer, and the rest are plate-type transducers. (**b**) At the bottom is the viscosity values of the systems (Reprinted from Ultrasonics Sonochemistry, 24, Nor Saadah Mohd Yusof, Muthupandian Ashokkumar, Ultrasonic transformation of micelle structures: Effect of frequency and power, 8–12 (2015), with permission from Elsevier)

known to increase with increasing power as the bubble size increases with an increase in power. Therefore, it can be expected that an increase in the micelle transformation from wormlike micelle to threadlike micelle occurs with increasing power, as shown in Fig. 20.

From Fig. 20, it can be seen that the shear forces generated at 10 W did not generate any structural changes in micelles. Sonication at 40 and 70 W results in the transformation of wormlike micelle and tubular micelle as observed before. The viscosity values increase with the increasing power. This supports the significant effect of shear in the formation of threadlike micelle from wormlike micelle upon sonication. The viscosity of the bottom layers did not show a significant change with increasing power from 40 to 70 W.

As also shown in the top left of Fig. 20, the sonication at 20 kHz of horn-type transducer results in only one phase of micelle, unlike the samples observed from

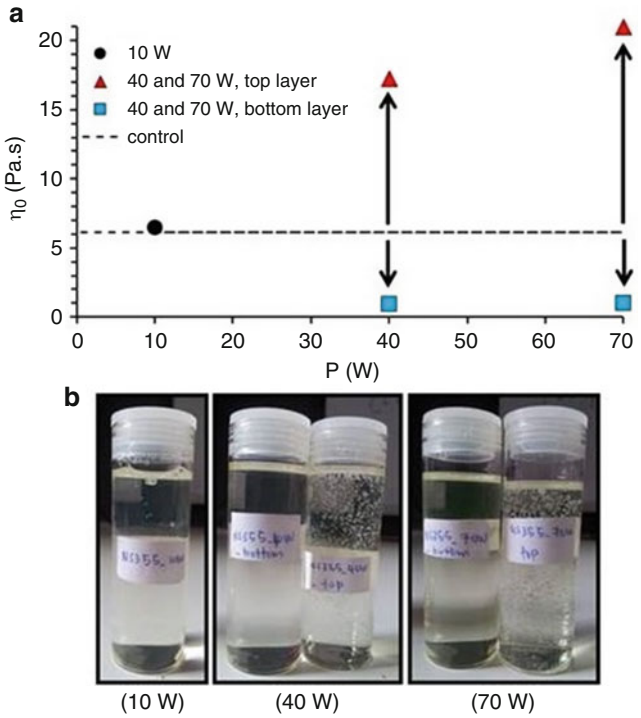

Fig. 20 The top is the viscosity values of CTASal micelle system at 355 kHz frequency and 10, 40, and 70 W of power. At the bottom are the images of the sonicated systems (Reprinted from Ultrasonics Sonochemistry, 24, Nor Saadah Mohd Yusof, Muthupandian Ashokkumar, Ultrasonic transformation of micelle structures: Effect of frequency and power, 8–12 (2015), with permission from Elsevier)

211 to 647 kHz. The viscosity was found to be at 3.3 Pa.s, about half of the original viscosity of CTASal before sonication. This is expected due to the very strong shear of such sonication system which may result in breaking of the micelles. The sonication using plate-type transducer at 1080 kHz also resulted in the formation of only one layer of micelle, with a much lower viscoelasticity observed. The viscosity value is just slightly above water (1.7 Pa.s) indicating the formation of vesicles and tubular micelles. As discussed earlier, the formation of long threadlike micelles take place through the reptation process of the wormlike micelles by the act of shear produced by the trapped oscillating microbubbles. On the other hand, when there are too many trapped microbubbles oscillating in opposite directions, the reptation process is disturbed, and micelle fragmentation occurs, resulting in the formation of disk-like micelles. They will then react together to form vesicles. A similar phenomenon is speculated at 1080 kHz. At this frequency, it is known that more microbubbles are formed by sonication, which may induce the formation of vesicles. This is supported by the viscosity value just above water shown.

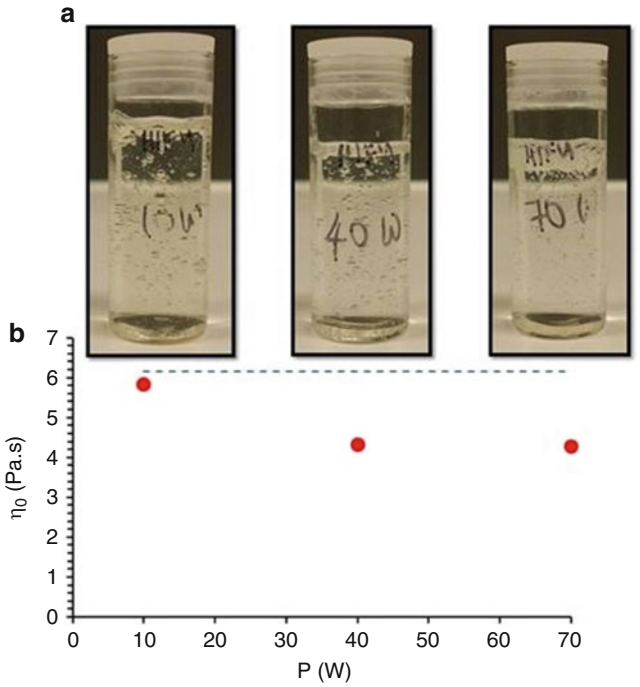

Fig. 21 (**a**) The images of sonicated CTASal micelle system using HIFU at 463 kHz frequency and applied power at 10, 40, and 70 W. (**b**) The viscosity values corresponding to (**a**)

Another type of sonicator used was the high-intensity focused ultrasound transducer, operated at 463 kHz frequency and at applied power of 10, 40, and 70 W. The pictures of the sonicated micelle system as well as their viscosity values are shown in Fig. 21.

As can be seen from Fig. 21, sonication of the micelle at all power levels results in only one phase of micelle. By visual observation, the viscoelasticity of these three systems cannot be distinguished. However, the viscosity values from rheological study showed a slight decrease in their viscosity in all three cases. We speculate that the breaking of CTASal micelles by HIFU took place, similar to the case proposed by Wang et al. [35] At 10 W, the viscosity was only slightly lower than the viscosity of CTASal before sonication. This is due to the weak shear forces generated below 25 W of power [64].

Conclusions and Future Directions

The basics of micelles and the effects of various stimuli on the structural and functional properties of micelles have been discussed in this chapter. The main focus of this chapter was to provide a comprehensive summary of the recently

completed study on the effect of ultrasound as a stimulus on the structural and functional properties of micelle systems. The data discussed in this chapter suggests that ultrasound can be used as an efficient stimulus in inducing micelle structural transformation in technological advancements. The following statements could be made from the data discussed in this chapter:

1. Ultrasonic irradiation of CTASal in the frequency range 211–647 kHz with power ranging from 10 to 70 W resulted in the transformation of wormlike micelle to long threadlike micelle and vesicle/tubular micelle, simultaneously.
2. According to the mechanism proposed, the direction of ultrasound-induced micellar changes and its extent of transformation are highly driven by the acoustic cavitation bubble oscillations.
3. The microbubble oscillation generates shear forces which drive the reptation process of the micelle. The temperature jump generated by microbubble implosion initiate recombination of micelles.
4. The transformation of CTASal micelle structure can be controlled by appropriate sonication experimental conditions as shown in Table 1. The structures are confirmed by the cryo-TEM images and rheological measurements.

The knowledge gained from this study can be applied in many technologies and applications. One of the examples is the Enhanced Oil Recovery (EOR) technology in oil drilling industry. In EOR technology, micelle with both behaviors of viscoelasticity and drag-reducing property are needed for different purposes. Therefore, both of the micelle characteristics are induced by different means of introducing different chemicals that does not only increase the cost of this industry, but could also be harmful to the environment. However, it is possible that by using ultrasound-induced micelle system, the required properties of micelle can be induced without the needs of introducing such harmful chemicals. If successful, this greener approach may eliminate the threats to the environment, as well as reduce the cost of EOR process.

References

1. Schryver SB et al (1913) Discussion. Trans Faraday Soc 9:93–107. doi:10.1039/TF9130900093
2. Croce V, Cosgrove T, Maitland G, Hughes T, Karlsson G (2003) Rheology, cryogenic transmission electron spectroscopy, and small-angle neutron scattering of highly viscoelastic wormlike micellar solutions. Langmuir 19:8536–8541. doi:10.1021/la0345800
3. Khatory A et al (1993) Entangled versus multiconnected network of wormlike micelles. Langmuir 9:933–939. doi:10.1021/la00028a010
4. Dreiss CA (2007) Wormlike micelles: where do we stand? Recent developments, linear rheology and scattering techniques. Soft Matter 3:956–970. doi:10.1039/B705775J
5. Guo L, Colby RH, Lin MY, Dado GP (2001) Micellar structure changes in aqueous mixtures of nonionic surfactants. J Rheol 45:1223–1243. doi:10.1122/1.1389315
6. Pérez-Juste J, Pastoriza-Santos I, Liz-Marzán LM, Mulvaney P (2005) Gold nanorods: synthesis, characterization and applications. Coord Chem Rev 249:1870–1901. doi:10.1016/j.ccr.2005.01.030

7. Vasudevan M, Shen A, Khomami B, Sureshkumar R (2008) Self-similar shear thickening behavior in CTAB/NaSal surfactant solutions. J Rheol 52:527–550. doi:10.1122/1.2833594
8. Yusof NSM, Khan MN (2010) Determination of an ion exchange constant by the use of a kinetic probe: a new semiempirical kinetic approach involving the effects of 3-F- and 4-F-substituted benzoates on the rate of piperidinolysis of anionic phenyl salicylate in aqueous cationic micelles. Langmuir 26:10627–10635. doi:10.1021/la100863q
9. Khan MN, Ismail E (2009) Kinetic evidence for the occurrence of independent ion-exchange processes in the cationic micellar-mediated reaction of piperidine with anionic phenyl salicylate. J Phys Chem A 113:6484–6488. doi:10.1021/jp902886z
10. Kim W-J, Yang S-M (2000) Effects of sodium salicylate on the microstructure of an aqueous micellar solution and its rheological responses. J Colloid Interface Sci 232:225–234. doi:10.1006/jcis.2000.7207
11. Magid LJ, Gee JC, Talmon Y (1990) A cryogenic transmission electron microscopy study of counterion effects on hexadecyltrimethylammonium dichlorobenzoate micelles. Langmuir 6:1609–1613. doi:10.1021/la00100a015
12. Arleth L, Bergström M, Pedersen JS (2002) Small-angle neutron scattering study of the growth behavior, flexibility, and intermicellar interactions of wormlike SDS micelles in NaBr aqueous solutions. Langmuir 18:5343–5353. doi:10.1021/la015693r
13. Magid LJ, Li Z, Butler PD (2000) Flexibility of elongated sodium dodecyl sulfate micelles in aqueous sodium chloride: a small-angle neutron scattering study. Langmuir 16:10028–10036. doi:10.1021/la0006216
14. Nakahara Y, Kida T, Nakatsuji Y, Akashi M (2005) New fluorescence method for the determination of the critical micelle concentration by photosensitive monoazacryptand derivatives. Langmuir 21:6688–6695. doi:10.1021/la050206j
15. Cates ME, Candau SJ (1990) Statics and dynamics of worm-like surfactant micelles. J Phys Condens Matter 2:6869
16. Cates ME (1990) Nonlinear viscoelasticity of wormlike micelles (and other reversibly breakable polymers). J Phys Chem 94:371–375. doi:10.1021/j100364a063
17. Magid LJ (1998) The surfactant−polyelectrolyte analogy. J Phys Chem B 102:4064–4074. doi:10.1021/jp9730961
18. Davies TS, Ketner AM, Raghavan SR (2006) Self-assembly of surfactant vesicles that transform into viscoelastic wormlike micelles upon heating. J Am Chem Soc 128:6669–6675. doi:10.1021/ja060021e
19. Koehler RD, Raghavan SR, Kaler EW (2000) Microstructure and dynamics of wormlike micellar solutions formed by mixing cationic and anionic surfactants. J Phys Chem B 104:11035–11044. doi:10.1021/jp0018899
20. Schubert BA, Kaler EW, Wagner NJ (2003) The microstructure and rheology of mixed cationic/anionic wormlike micelles. Langmuir 19:4079–4089. doi:10.1021/la020821c
21. Candau SJ, Hirsch E, Zana R (1985) Light scattering investigations of the behavior of semidilute aqueous micellar solutions of cetyltrimethylammonium bromide: analogy with semidilute polymer solutions. J Colloid Interface Sci 105:521–528. doi:10.1016/0021-9797(85)90327-3
22. Magid LJ, Han Z, Li Z, Butler PD (2000) Tuning microstructure of cationic micelles on multiple length scales: the role of electrostatics and specific ion binding. Langmuir 16:149–156. doi:10.1021/la990686c
23. Raghavan SR, Kaler EW (2000) Highly viscoelastic wormlike micellar solutions formed by cationic surfactants with long unsaturated tails. Langmuir 17:300–306. doi:10.1021/la0007933
24. Khatory A, Lequeux F, Kern F, Candau SJ (1993) Linear and nonlinear viscoelasticity of semidilute solutions of wormlike micelles at high salt content. Langmuir 9:1456–1464. doi:10.1021/la00030a005
25. Clausen TM et al (1992) Viscoelastic micellar solutions: microscopy and rheology. J Phys Chem 96:474–484. doi:10.1021/j100180a086

26. Gravsholt S (1976) Viscoelasticity in highly dilute aqueous solutions of pure cationic detergents. J Colloid Interface Sci 57:575–577. doi:10.1016/0021-9797(76)90236-8
27. Hassan PA et al (1996) Vesicle to micelle transition: rheological investigations. Langmuir 12:4350–4357
28. Mendes E et al (1997) Shear-induced vesicle to wormlike micelle transition. J Phys Chem B 101:2256–2258. doi:10.1021/jp962790y
29. Mahmood ME, Al-Koofee DAF (2013) Effect of temperature changes on critical micelle concentration for tween series surfactant. Glob J Sci Front Res Chem 13:1–7
30. Mendes E et al (1997) Shear-induced vesicle to wormlike micelle transition. J Phys Chem B 101:2256–2258
31. Prötzl B, Springer J (1997) Light scattering experiments on shear induced structures of micellar solutions. J Colloid Interface Sci 190:327–333. doi:10.1006/jcis.1997.4866
32. Chen S, Rothstein JP (2004) Flow of a wormlike micelle solution past a falling sphere. J Non-Newtonian Fluid Mech 116:205–234. doi:10.1016/j.jnnfm.2003.08.005
33. Cressely R, Hartmann V (1998) Rheological behaviour and shear thickening exhibited by aqueous CTAB micellar solutions. Eur Phys J B 6:57–62. doi:10.1007/s100510050526
34. Zheng Y et al (2000) Cryo-TEM imaging the flow-induced transition from vesicles to threadlike micelles. J Phys Chem B 104:5263–5271. doi:10.1021/jp0002998
35. Wang J, Pelletier M, Zhang H, Xia H, Zhao Y (2009) High-frequency ultrasound-responsive block copolymer micelle. Langmuir 25:13201–13205. doi:10.1021/la9018794
36. Pitt WG, Husseini GA, Staples BJ (2004) Ultrasonic drug delivery – a general review. Expert Opin Drug Deliv 1:37–56. doi:10.1517/17425247.1.1.37
37. Kost J, Leong K, Langer R (1989) Ultrasound-enhanced polymer degradation and release of incorporated substances. Proc Natl Acad Sci 86:7663–7666
38. Ghosh S et al (2013) Spontaneous transition of micelle–vesicle–micelle in a mixture of cationic surfactant and anionic surfactant-like ionic liquid: a pure nonlipid small unilamellar vesicular template used for solvent and rotational relaxation study. Langmuir 29:10066–10076. doi:10.1021/la402053a
39. Miskolczy Z, Sebők-Nagy K, Biczók L, Göktürk S (2004) Aggregation and micelle formation of ionic liquids in aqueous solution. Chem Phys Lett 400:296–300. doi:10.1016/j.cplett.2004.10.127
40. Silva BFB, Marques EF (2005) Thermotropic behavior of asymmetric chain length catanionic surfactants: the influence of the polar head group. J Colloid Interface Sci 290:267–274. doi:10.1016/j.jcis.2005.04.012
41. Kaler EW, Murthy AK, Rodriguez BE, Zasadzinski JA (1989) Spontaneous vesicle formation in aqueous mixtures of single-tailed surfactants. Science 245:1371–1374
42. Yatcilla MT et al (1996) Phase behavior of aqueous mixtures of cetyltrimethylammonium bromide (CTAB) and sodium octyl sulfate (SOS). J Phys Chem 100:5874–5879. doi:10.1021/jp952425r
43. Marques EF (2000) Size and stability of catanionic vesicles: effects of formation path, sonication, and aging. Langmuir 16:4798–4807. doi:10.1021/la9908135
44. Yusof NSM, Ashokkumar M (2013) Ultrasound-induced formation of high and low viscoelastic nanostructures of micelles. Soft Matter 9:1997–2002. doi:10.1039/C2SM27423J
45. Cates ME (1987) Reptation of living polymers: dynamics of entangled polymers in the presence of reversible chain-scission reactions. Macromolecules 20:2289–2296. doi:10.1021/ma00175a038
46. Messager R, Ott A, Chatenay D, Urbach W, Langevin D (1988) Are giant micelles living polymers? Phys Rev Lett 60:1410–1413
47. de Gennes PG (1971) Reptation of a polymer chain in the presence of fixed obstacles. J Chem Phys 55:572–579. doi:10.1063/1.1675789
48. Leger L, Hervet H, Rondelez F (1981) Reptation in entangled polymer solutions by forced Rayleigh light scattering. Macromolecules 14:1732–1738

49. Tanford C (1974) Theory of micelle formation in aqueous solutions. J Phys Chem 78:2469–2479. doi:10.1021/j100617a012
50. Turner MS, Marques C, Cates ME (1993) Dynamics of wormlike micelles: the "bond-interchange" reaction scheme. Langmuir 9:695–701. doi:10.1021/la00027a015
51. Candau SJ, Hirsch E, Zana R, Adam M (1988) Network properties of semidilute aqueous KBr solutions of cetyltrimethylammonium bromide. J Colloid Interface Sci 122:430–440. doi:10.1016/0021-9797(88)90377-3
52. Wunderlich I, Hoffmann H, Rehage H (1987) Flow birefringence and rheological measurements on shear induced micellar structures. Rheol Acta 26:532–542. doi:10.1007/BF01333737
53. Rehage H, Hoffmann H (1988) Rheological properties of viscoelastic surfactant systems. J Phys Chem 92:4712–4719. doi:10.1021/j100327a031
54. Leger L, Hervet H, Rondelez F (1981) Reptation in entangled polymer solutions by forced Rayleigh light scattering. Macromolecules 14:1732–1738. doi:10.1021/ma50007a023
55. Ashokkumar M, Mason TJ (2000) In: Kirk-Othmer encyclopedia of chemical technology. Wiley
56. Leighton T (1994) Academic Press, London
57. Tho P, Manasseh R, Ooi A (2007) Cavitation microstreaming patterns in single and multiple bubble systems. J Fluid Mech 576:191–233. doi:10.1017/S0022112006004393
58. Shoh A (1975) Industrial applications of ultrasound – a review I. High-power ultrasound. IEEE Trans Sonics Ultrason 22:60–70. doi:10.1109/T-SU.1975.30780
59. Patist A, Jha BK, Oh S g, Shah DO (1999) Importance of micellar relaxation time on detergent properties. J Surfactant Deterg 2:317–324. doi:10.1007/s11743-999-0083-6
60. Ziserman L, Abezgauz L, Ramon O, Raghavan SR, Danino D (2009) Origins of the viscosity peak in wormlike micellar solutions. 1. mixed catanionic surfactants. A cryo-transmission electron microscopy study. Langmuir 25:10483–10489. doi:10.1021/la901189k
61. Mohanty A, Patra T, Dey J (2007) Salt-induced vesicle to micelle transition in aqueous solution of sodium *N*-(4-n-octyloxybenzoyl)-l-valinate. J Phys Chem B 111:7155–7159. doi:10.1021/jp071312s
62. Brotchie A, Grieser F, Ashokkumar M (2009) Effect of power and frequency on bubble-size distributions in acoustic cavitation. Phys Rev Lett 102:084302
63. Ashokkumar M, Maspm TJ (2007) In: Kirk Othmer encyclopedia chemical tenchnology
64. Yusof NSM, Ashokkumar M (2015) Ultrasonic transformation of micelle structures: effect of frequency and power. Ultrason Sonochem. 24:8–12. doi:10.1016/j.ultsonch.2014.11.003